JOURNAL OF COMPUTATIONAL PHYSICS **127,** 208–217 (1996)
ARTICLE NO. 0169

Optimal Vorticity Conditions for the Node-Centred Finite-Difference Discretization of the Second-Order Vorticity–Velocity Equations

P. GIANNATTASIO* AND M. NAPOLITANO†

*Dipartimento di Energetica e Macchine, Universitá di Udine, Via Delle Scienze 208, 33100 Udine, Italy; and †Istituto di Macchine ed Energetica, Politecnico di Bari, Via Re David 200, 70125 Bari, Italy

Received March 27, 1995; revised March 22, 1996

The present paper considers the 2D vorticity–velocity Navier–Stokes equations written as a second-order system, when a node-centred finite-difference discretization and a uniform Cartesian grid are employed. For such a formulation common vorticity boundary conditions yield much inferior solutions to those obtained in the node-centred vorticity–stream function or staggered-grid vorticity–velocity formulations. However, we demonstrate that these three formulations are formally equivalent in the sense that they all identically satisfy: (i) the node-centred finite-difference form of the continuity equation; (ii) the node-centred finite-difference form of the vorticity definition with respect to the mid-cell or staggered velocity components; and (iii) the cell-centred finite-volume (integral) form of the vorticity definition with respect to the nodal values of the velocity components. This last property naturally provides the ''optimal'' boundary conditions for the wall vorticity in the node-centred vorticity–velocity formulation. Numerical solutions to the driven cavity flow problem are provided which confirm the equivalence of the three formulations.

1. INTRODUCTION

Numerical solutions to the vorticity–velocity (ω, $\mathbf{V}$) Navier–Stokes equations have been pioneered by Fasel [1] to study the stability of 2D boundary layers. Successively, many researchers have used such equations for calculating 2D and 3D steady [2–7] as well as unsteady [8, 9] flows. In particular, when the continuity equation and the vorticity definition are replaced with a Poisson equation for the velocity vector, the resulting second-order system for ω and $\mathbf{V}$ is very similar to that for the vorticity and the stream function (ψ) in two dimensions. One can thus employ numerical methods which proved to be successful for such a formulation [6, 7].

Unfortunately, the numerical solutions to the second-order ω, $\mathbf{V}$ system satisfy the discrete counterparts of the continuity equation and of the vorticity definition only when using a staggered-grid discretization [4, 7, 9]. On the contrary, if one uses a node-centred discretization, some nontrivial difficulties arise, as shown in Refs. [5, 6]. The numerical solutions are extremely sensitive to the approximation of the equation $\omega = \text{curl } \mathbf{V}$, used at solid walls to provide a substitute for the missing boundary condition for the vorticity. Furthermore, although a second-order-accurate compact discretization [5, 6] of such a vorticity definition provides satisfactory solutions for a wide range of the Reynolds number [6], the discrete counterpart of $\text{div } \mathbf{V} = 0$ obtained from such solutions goes to zero less than linearly with the mesh size h for h as small as 0.005. Nevertheless, the greater simplicity of a node-centred scheme, particularly in view of the 3D equations and when combined with a multigrid (see Refs. [6, 7] for details) justifies a continuing effort to circumvent the aforementioned difficulties.

To this end, the following numerical experiment was performed. The 2D node-centred vorticity–velocity equations (ω, u, v) were solved using the vorticity boundary values obtained from the solution of the ω, ψ equations on the same grid. The entire vorticity field was identical to that of the ω, ψ solution as anticipated, and, more importantly, the velocity field turned out to be numerically divergence-free to machine accuracy. Therefore, a study was undertaken, aimed at discovering appropriate numerical boundary conditions for the vorticity capable of providing such a divergence-free solution [10]. In that study, the velocity field was integrated numerically along each gridline so as to reproduce the same formula for ω at the wall used with success in the ω, ψ formulation. For the case of grids having an even number of gridpoints in both spatial directions the approach easily provided the sought solution, whereas for the case of an odd number of gridpoints a different divergence-free numerical solution was obtained for each choice of an arbitrary constant. Most likely, among all such solutions there was the one sought, but no practical means of obtaining it was devised.

Nevertheless, the goal of making the node-centred finite-difference solution to the second-order ω, u, v system as accurate as the corresponding staggered-grid one appeared within reach. Therefore, a comparative analysis of the node-centred and staggered-grid ω, u, v formulations, as well as of the ω, ψ one, has been carried out in this paper. In the following sections, it will be shown that these three formulations can satisfy exactly the discrete counterpart

0021-9991/96 $18.00

of the differential continuity equation. Moreover, they can satisfy exactly the discrete vorticity definition, $\boldsymbol{\omega} = \text{curl } \mathbf{V}$, with respect to the mid-cell velocity components. Finally, they can satisfy exactly the discrete form of the integral definition of vorticity, as provided by a local application of Stokes' theorem, with respect to the nodal values of the velocity components. Most importantly, by using such an integral vorticity definition at the boundary cells, one obtains the long-sought numerical condition at no-slip boundaries, which makes the node-centred ω, u, v formulation equivalent to the staggered-grid one.

After describing how to modify an existing numerical method for the node-centred ω, u, v equations, in order to implement the new numerical boundary conditions for the vorticity, solutions to the classical driven cavity problem [11] are presented which validate the proposed approach.

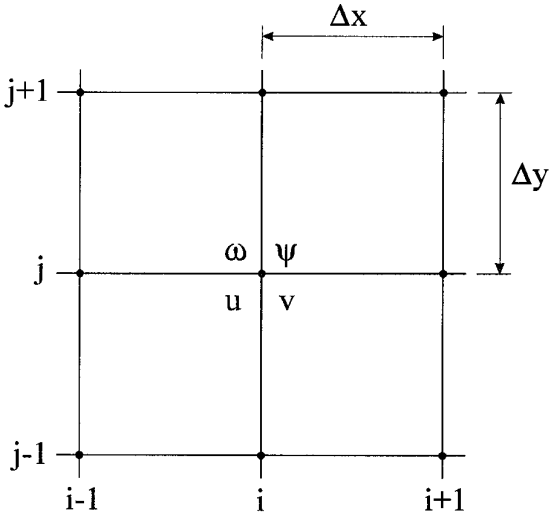

FIG. 1. Node-centred grid used for the ω, ψ, and ω, u, v formulations.

2. GOVERNING EQUATIONS

The 2D vorticity–velocity Navier–Stokes equations can be formulated in Cartesian coordinates (x, y) as

$$\omega_t + (u\omega)_x + (v\omega)_y = \frac{1}{\text{Re}}(\omega_{xx} + \omega_{yy}), \tag{1}$$

$$u_{xx} + u_{yy} = -\omega_y, \tag{2}$$

$$v_{xx} + v_{yy} = \omega_x, \tag{3}$$

where t is the time, u and v are the two components of the velocity vector $\mathbf{V}$, Re is the Reynolds number, the advection terms are written in conservative form, and the subscripts denote partial derivatives.

In Eqs. (1)–(3) the two Poisson equations for u and v are derived from the continuity equation and the definition of vorticity, namely,

$$u_x + v_y = 0, \tag{4}$$

$$\omega = v_x - u_y. \tag{5}$$

In the following, it will be useful to consider the ω, ψ formulation of the incompressible Navier–Stokes equations, which is recalled here for convenience:

$$\omega_t + (\psi_y\omega)_x - (\psi_x\omega)_y = \frac{1}{\text{Re}}(\omega_{xx} + \omega_{yy}), \tag{6}$$

$$\psi_{xx} + \psi_{yy} = -\omega. \tag{7}$$

Concerning the no-slip boundary conditions to be imposed at solid walls, one has: (i) for the ω, u, v formulation, both velocity components are prescribed; (ii) for the ω, ψ formulation, the values of ψ and of its normal derivative are provided. In both cases, no boundary condition is available for ω. The value of ω at boundary gridpoints is thus evaluated in the first case using its definition [1–7], $\omega = \text{curl } \mathbf{V}$, and in the second case by means of a combination of the Neumann condition for ψ and of Eq. (7) (see, e.g., Ref. [11]) as described in the following.

3. NUMERICAL BOUNDARY CONDITIONS

As already mentioned in the Introduction, three discrete formulations of the 2D incompressible Navier–Stokes equations are considered in this paper, namely, the node-centred and staggered-grid ω, u, v formulations and the (node-centred) ω, ψ one. The uniform Cartesian grids employed by the node-centred and staggered-grid formulations are shown in Figs. 1 and 2, where the locations of the various variables are indicated, and in Figs. 3a–c, where solid-wall boundaries are represented.

Concerning the ω, ψ and the staggered-grid ω, u, v formulations, the no-slip boundary conditions are given, respectively, as

$$\psi_1 = a, \quad \frac{\psi_2 - \psi_0}{2\Delta y} = b, \quad \omega_1 = -\frac{\psi_2 - 2\psi_1 + \psi_0}{\Delta y^2}, \tag{8a), (8b), (8c)}$$

$$\frac{u_{3/2} + u_{1/2}}{2} = b, \quad \omega_1 = -\frac{u_{3/2} - u_{1/2}}{\Delta y}. \tag{9a), (9b)}$$

In Eqs. (8) and (9), the discrete counterparts of ψ_{xx} and v_x at the wall are omitted, being identically zero; a and b are the prescribed wall values of ψ and u; and subscripts 0 and $\frac{1}{2}$ refer to the mirror points outside the computational domain [7, 11] shown in Figs. 3a, b.

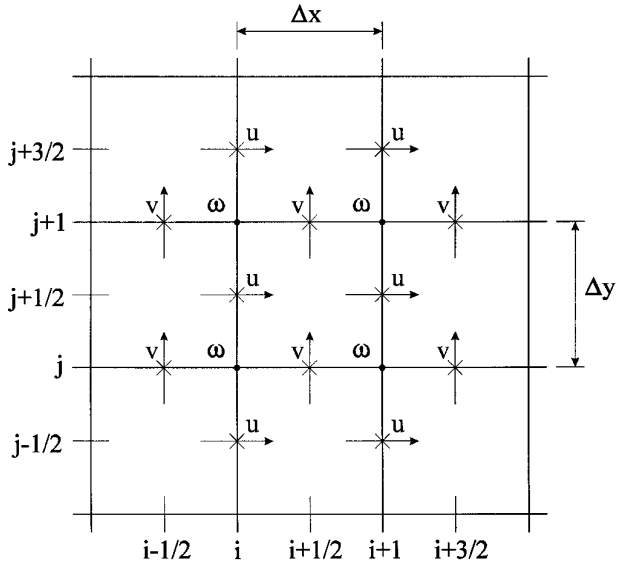

FIG. 2. Staggered-grid used for the ω, u, v formulation.

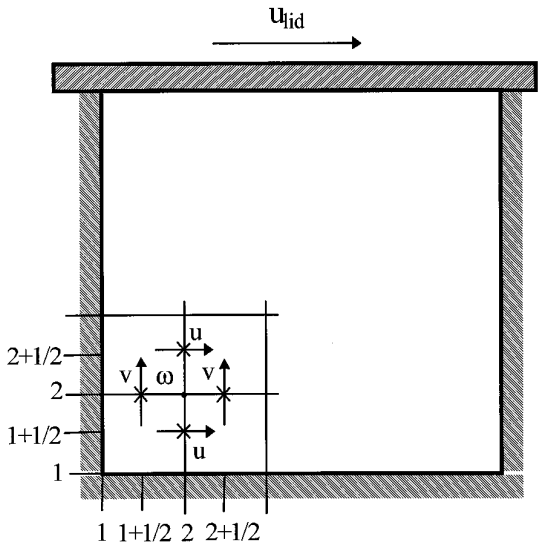

FIG. 4. Driven cavity geometry and local grid near the bottom-left corner.

For the case of the node-centred ω, u, v formulation, of major interest here, it has been shown that the space discretization used to evaluate Eq. (5) at solid boundaries has a critical impact on the quality of the numerical solution [5, 6]. In particular, with reference to Fig. 3a, the following two second-order-accurate discretizations of Eq. (5) are used in this study:

$$\omega_1 = \frac{-u_3 + 4u_2 - 3u_1}{2\Delta y}, \tag{10}$$

$$\frac{\omega_1 + \omega_2}{2} = -\frac{u_2 - u_1}{\Delta y}. \tag{11}$$

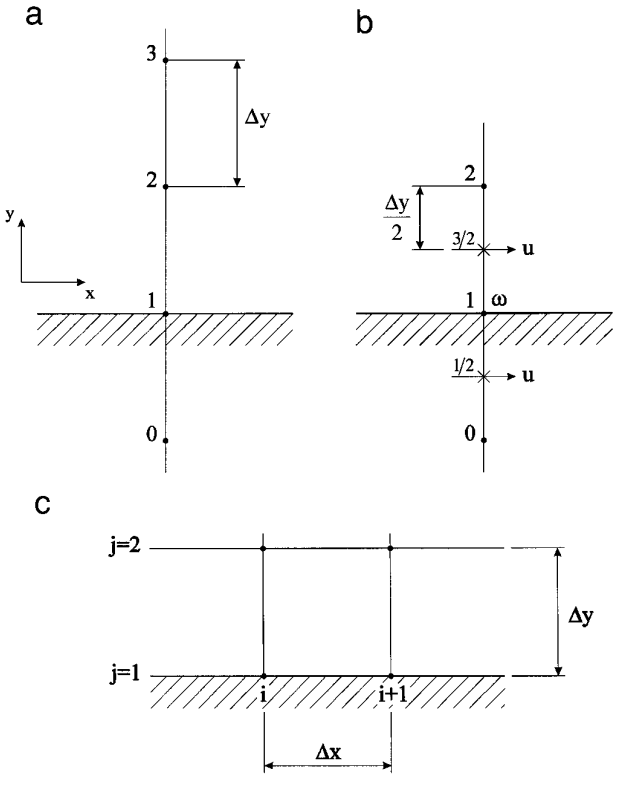

FIG. 3. Near wall grids considered for the various numerical vorticity boundary conditions.

For the driven-cavity flow problem [11] at Re = 400 (see Fig. 4) numerical solutions have been obtained using a second-order-accurate node-centred spatial discretization, the conservative form of the advection terms in the vorticity transport equation and either Eq. (10) or Eq. (11) to evaluate ω at all boundary points (except the four corner points, which do not need to be computed). The u and v profiles along the vertical and horizontal centerlines of the cavity are provided in Fig. 5 for a uniform 49×49 grid ($\Delta x = \Delta y = h = \frac{1}{48}$). The dotted and broken lines refer to the Eq. (10)-solution and the Eq. (11)-solution, respectively, whereas the solid line refers to the staggered-grid solution, which is identical to the node-centred solution of the ω, ψ equations [4, 7]. The superiority of Eq. (11), with respect to Eq. (10), is paramount and the inadequacy of the latter is worrisome insofar as the problem under consideration should be well captured by the grid used. However, if one refines the grid, the two solutions become much closer to each other (see Fig. 6) which provides the three sets of results for the case of a uniform 193×193 grid ($h = \frac{1}{192}$).

The corresponding vorticity distributions along the moving lid of the cavity are also given in Figs. 7 and 8, for

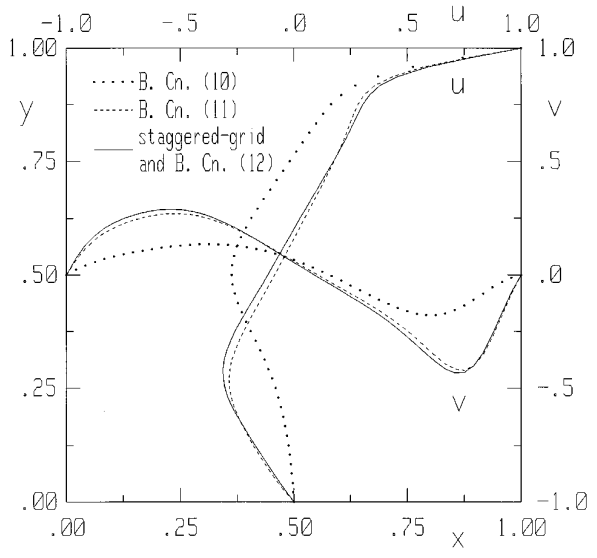

FIG. 5. Velocity distributions along the centerlines of the cavity for Re = 400 and $h = \frac{1}{48}$ (the solid lines also refer to the ω, ψ solution).

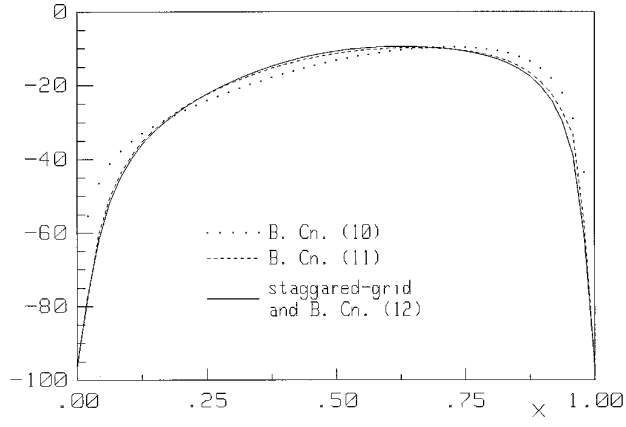

FIG. 7. Vorticity distributions along the lid of the cavity for Re = 400 and $h = \frac{1}{48}$ (the solid line also refers to the ω, ψ solution).

completeness. It clearly appears that, whereas the wall vorticity is always reasonable, the interior velocity field is seriously compromised by its nonzero divergence.

The numerical difficulty described above has been overcome in this paper by using a novel numerical condition for the wall vorticity, which makes the node-centred ω, u, v formulation identical in the discrete to the staggered one and thus also to the ω, ψ formulation. Such a novel numerical condition is nothing but the second-order-accurate compact-stencil approximation of Stokes' theorem applied to each boundary cell. With reference to the cell in Fig. 3c, it reads

$$\frac{\omega_{i,1} + \omega_{i+1,1} + \omega_{i,2} + \omega_{i+1,2}}{4} \Delta x \, \Delta y = \left(\frac{v_{i+1,1} + v_{i+1,2}}{2} - \frac{v_{i,1} + v_{i,2}}{2} \right) \Delta y + \left(\frac{u_{i,1} + u_{i+1,1}}{2} - \frac{u_{i,2} + u_{i+1,2}}{2} \right) \Delta x. \tag{12}$$

Discovering such an apparently trivial, but very important, numerical boundary condition was made possible by the analysis described in the following section. Here, it is anticipated that using such "optimal" numerical boundary condition for ω in the collocated ω, u, v formulation provided the same results as the staggered-grid ones, shown

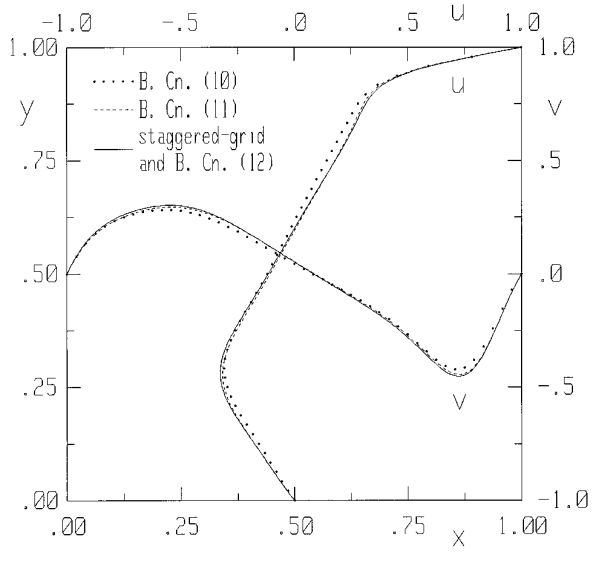

FIG. 6. Velocity distributions along the centerlines of the cavity for Re = 400 and $h = \frac{1}{192}$ (the solid lines also refer to the ω, ψ solution).

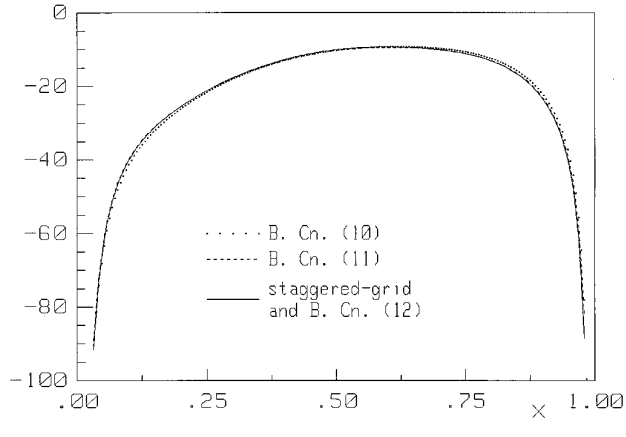

FIG. 8. Vorticity distributions along the lid of the cavity for Re = 400 and $h = \frac{1}{192}$ (the solid line also refers to the ω, ψ solution).

in Figs. 5–8 as solid lines. More importantly, these results satisfy the discrete counterpart of the continuity equation (4) exactly, i.e., to machine accuracy.

It is noteworthy that for 1D flows Eq. (12) degenerates into Eq. (11). This may explain the superiority of Eq. (11) with respect to Eq. (10).

4. A COMPARATIVE ANALYSIS OF THE ω, u, v AND ω, ψ FORMULATIONS

In this section, the node-centred and staggered-grid ω, u, v formulations, as well as the ω, ψ one, are analyzed with reference to second-order-accurate central-difference discretizations on uniform Cartesian grids.

Consider the node-centred discretization of Eq. (2) at gridpoint (x_i, y_j), namely,

$$\frac{\omega_{i,j+1} - \omega_{i,j-1}}{2\Delta y} = -\frac{u_{i+1,j} - 2u_{i,j} + u_{i-1,j}}{\Delta x^2} - \frac{u_{i,j+1} - 2u_{i,j} + u_{i,j-1}}{\Delta y^2}. \tag{13}$$

Eliminate the ω terms in Eq. (13) by means of the discrete form of the vorticity definition (5),

$$\omega_{i,j} = \frac{v_{i+1,j} - v_{i-1,j}}{2\Delta x} - \frac{u_{i,j+1} - u_{i,j-1}}{2\Delta y}. \tag{14}$$

Then, express the v velocity components in the resulting numerical equation in terms of the u velocity components, by using the discrete form of the continuity equation (4),

$$\frac{u_{i+1,j} - u_{i-1,j}}{2\Delta x} + \frac{v_{i,j+1} - v_{i,j-1}}{2\Delta y} = 0, \tag{15}$$

written at nodes (x_{i+1}, y_j) and (x_{i-1}, y_j). If Eq. (13) were numerically equivalent to the discrete counterparts of Eqs. (4) and (5), the resulting equation should be an identity. Unfortunately, this is not the case, since the following nonzero residual term is obtained:

$$\begin{aligned}\delta_{i,j} &= (u_{i+2,j} - 4u_{i+1,j} + 6u_{i,j} - 4u_{i-1,j} + u_{i-2,j})/4\Delta x^2 \\ &\quad + (u_{i,j+2} - 4u_{i,j+1} + 6u_{i,j} - 4u_{i,j-1} + u_{i,j-2})/4\Delta y^2 \\ &= \frac{\Delta x^2}{4}(u_{xxxx})_{i,j} + \frac{\Delta y^2}{4}(u_{yyyy})_{i,j} + O(\Delta x^4, \Delta y^4).\end{aligned} \tag{16}$$

A similar term comes out when one starts from the Poisson equation (3). It is noteworthy that the $\delta_{i,j}$ term in Eq. (16) is formally identical to that obtained by Sotiropoulos and Abdallah [12] for the pressure equation, when considering a node-centred discretization of the primitive variable formulation of the Navier–Stokes equations. As in Ref. [12], one could think of subtracting these terms explicitly from the discrete Poisson equations (2) and (3) in order to obtain a numerical solution satisfying both discrete equations (4) and (5). Unfortunately, this leads to an even–odd decoupling of the Poisson equations, which cannot thus be solved numerically.

From the analysis above, it is clear that the node-centred solutions of Eqs. (1)–(3) cannot satisfy exactly the discrete counterparts of both Eqs. (4) and (5). However, it can be shown (see Appendix A) that, if the solutions of the node-centred ω, ψ and ω, u, v equations provide identical discrete vorticity fields, they satisfy the relationships

$$u_{i,j} = \frac{\psi_{i,j+1} - \psi_{i,j-1}}{2\Delta y}, \tag{17}$$

$$v_{i,j} = -\frac{\psi_{i+1,j} - \psi_{i-1j}}{2\Delta x}. \tag{18}$$

Namely, from the identity of the two vorticity fields it follows that the velocity fields are also equivalent. In particular, the ω, u, v solution turns out to be exactly divergence-free (it can be easily verified by expressing the velocity components in Eq. (15) in terms of nodal values of ψ, according to Eqs. (17) and (18)), but it does not satisfy the discrete form of Eq. (5) exactly, as already shown when the residual term in Eq. (16) was singled out. On the other hand, the equivalent ω, ψ solution satisfies such an equation, exactly, with reference to the mid-cell velocity components, namely,

$$u_{i,j+1/2} = \frac{\psi_{i,j+1} - \psi_{i,j}}{\Delta y}, v_{i+1/2,j} = -\frac{\psi_{i+1,j} - \psi_{i,j}}{\Delta x}.$$

This result is an obvious consequence of the equivalence of the ω, ψ and staggered-grid ω, u, v formulations, proven in Refs. [4, 7]. Therefore, the ω, ψ solution turns out to be equivalent to both the node-centred and staggered-grid ω, u, v solutions, which provide identical vorticity fields. Moreover, the discrete velocity fields obtained from these two ω, u, v solutions satisfy

$$u_{i,j} = \frac{u_{i,j+1/2} + u_{i,j-1/2}}{2}, \tag{19}$$

$$v_{i,j} = \frac{v_{i+1/2,j} + v_{i-1/2,j}}{2}, \tag{20}$$

as demonstrated in Appendix B. Finally, provided the staggered-grid ω, u, v solution satisfies

$$\omega_{i,j} = \frac{v_{i+1/2,j} - v_{i-1/2,j}}{\Delta x} - \frac{u_{i,j+1/2} - u_{i,j-1/2}}{\Delta y} \tag{21}$$

at all gridpoints, it follows that the corresponding node-centred ω, u, v solution satisfies

$$\frac{\omega_{i,j} + \omega_{i+1,j} + \omega_{i,j+1} + \omega_{i+1,j+1}}{4} \Delta x\, \Delta y = \left(\frac{v_{i+1,j} + v_{i+1,j+1}}{2} - \frac{v_{i,j} + v_{i,j+1}}{2} \right) \Delta y + \left(\frac{u_{i,j} + u_{i+1,j}}{2} - \frac{u_{i,j+1} + u_{i+1,j+1}}{2} \right) \Delta x. \tag{22}$$

This result is proven in Appendix C. It is noteworthy that Eq. (22) is the compact-stencil second-order-accurate discrete approximation of the integral condition

$$\iint_{\Delta S} \omega dS = \oint_{l} \mathbf{V} \cdot \boldsymbol{\tau}\, dl, \tag{23}$$

namely, of Stokes' theorem applied to the computational cell $[x_i, x_{i+1}] \times [y_j, y_{j+1}]$.

In conclusion, the node-centred ω, ψ and ω, u, v solutions are both equivalent to the staggered-grid ω, u, v solution, in the sense that they all satisfy identically the discrete counterparts of: (i) the differential form of the continuity equation; (ii) the differential form of the vorticity definition with respect to the mid-cell velocity components; (iii) the integral form of the vorticity definition with respect to the nodal values of the velocity components.

The important practical consequence of proving this equivalence is that, by writing Eq. (22) at all computational cells neighboring no-slip boundaries (see Eq. (12)), one obtains the ''optimal'' numerical condition for the wall vorticity, namely, the one which renders the node-centred ω, u, v solution equivalent to the staggered-grid one.

It is very important to realize that there is a topological difficulty associated with the use of the numerical vorticity conditions (12) within the context of a collocated space discretization; namely, the number of Eqs. (12), which is equal to that of the boundary cells, is not always equal to the number of boundary gridpoints at which ω is to be determined. For a Cartesian domain, of interest here, it is easily seen that the boundary gridpoints outnumber the boundary cells by the number of convex (90°) interior corners. This is not a problem because, due to the no-slip conditions on the horizontal and vertical sides of the boundary meeting at such a corner, the local vorticity must equal zero. On the other hand, it is possible to obtain the additional equations which allow us to evaluate the vorticity values at all the boundary points, including the convex corners, as shown in the next section for the very peculiar case of the driven cavity problem [11].

Finally, it must be clearly pointed out that the proposed numerical boundary conditions for the vorticity, although using a local area integral, have nothing in common with the well-known vorticity integral conditions of Quartapelle [13]. The latter ones allow us to decouple the governing equations, apart from the nonlinear advection terms, so that the vorticity at solid boundaries is determined solely by means of the velocity boundary conditions. In the present approach, the vorticity at solid walls requires the knowledge of the vorticity and velocity values at points on the boundary and immediately adjacent to it. Therefore, the use of the proposed conditions requires a coupled or iterative solution procedure, as described in the following section.

5. NUMERICAL IMPLEMENTATION

In order to show how the wall vorticity conditions derived in the previous section can be imposed in practice, the classical driven cavity flow problem is considered, using a uniform $m \times n$ grid with $\Delta x = 1/(m-1)$ and $\Delta y = (1/(n-1)$. Of course, the u and v velocity components are prescribed at all boundary points, $v_{i,1} = v_{1,j} = v_{i,n} = v_{m,j} = u_{i,1} = u_{1,j} = u_{m,j} = 0$, $u_{i,n} = 1$, $i = 1, ..., m$; $j = 2, ..., n-1$, thus providing $4(m + n - 2)$ boundary conditions. The governing equations (1)–(3), discretized at all the internal nodes provide $3(m-2)(n-2)$ equations in $3mn$ unknowns. Equation (12) is then employed for all boundary cells, thus providing $2(m + n - 4)$ algebraic equations containing the $2(m + n - 2)$ vorticity boundary values. The four missing equations can be finally obtained by resorting once again to the proven equivalence of the staggered-grid and node-centred ω, u, v formulations. Such equations, derived as shown in Appendix D, are given by

$$\omega_{1,2} = \frac{2(v_{2,2}/\Delta x - u_{2,2}/\Delta y) - \omega_{2,2}}{1 + (\Delta x/\Delta y)^2}, \tag{24a}$$

$$\omega_{2,n} = \frac{2(v_{2,n-1}/\Delta x + u_{2,n-1}/\Delta y) - \omega_{2,n-1}}{1 + (\Delta y/\Delta \mathrm{x})^2} - \frac{2}{\Delta y} u_{\mathrm{lid}}, \tag{24b}$$

$$\omega_{m,n-1} = -\frac{2(v_{m-1,n-1}/\Delta x - u_{m-1,n-1}/\Delta y) + \omega_{m-1,n-1}}{1 + (\Delta x/\Delta y)^2}, \tag{24c}$$

$$\omega_{m-1,1} = -\frac{2(v_{m-1,2}/\Delta x + u_{m-1,2}/\Delta y) + \omega_{m-1,2}}{1 + (\Delta y/\Delta x)^2}. \tag{24d}$$

The discrete system to be solved is now closed, since there are $3mn$ equations in $3mn$ unknowns. It is noteworthy that the four corner vorticities appear only in the four equations (12) written at the corner cells. Therefore, it is possible to remove these four equations and unknowns so as to obtain a reduced closed system of $3mn - 4$ equations in $3mn - 4$ unknowns. After solving such a system, as described later, the vorticities at the four corners can be evaluated explicitly using Stokes' theorem, exactly like one does

when solving the ω, ψ equations or the staggered-grid ω, u, v equations. The equivalence of the three formulations is thus complete, even in such an apparently minor detail.

From the preceding discussion, it follows that there are two possibilities of implementing the proposed vorticity condition within the context of an iterative solution procedure. By evaluating all internal vorticities and velocities in Eqs. (12) and (24) at the previous iteration, one decouples them from all other equations written at the internal points. Then, if one enforces the four known vorticity values at the corners, one uses all $2(m + n - 4)$ equations (12) to evaluate the remaining $2(m + n - 4)$ vorticity boundary values, by solving a periodic bidiagonal system. If one prefers the more general approach of eliminating the four corner vorticities from the problem, it turns out that the $2(m + n - 6)$ equations (12) not containing the corner values plus the four equations (24) can be solved explicitly.

It must be pointed out that the numerical solution obtained using either procedure described above does satisfy the discrete integral definition of the vorticity, Eq. (22), also at all nonboundary cells and, therefore, also over the entire computational domain.

6. NUMERICAL METHOD AND RESULTS

In order to test the proposed formulation, a reliable and efficient numerical method [6] has been used to solve the driven cavity flow problem. The method is a scalar alternating direction line-Gauss–Seidel iterative procedure accelerated by multigrid. The vorticity at all the boundary gridpoints is evaluated explicitly before each solution sweep, using the procedure described in the previous section.

Since the present calculations have the sole purpose of validating the numerical vorticity boundary conditions, the results are presented for the single case Re = 400, using $h = \frac{1}{48}$ and $h = \frac{1}{192}$. Convergence to machine zero, using single-precision arithmetic, has been obtained. As anticipated, the two vorticity fields obtained using the present approach and the staggered-grid method of Ref. [7] were found to be identical within roundoff. Furthermore, the corresponding velocity fields have been verified to satisfy Eqs. (19) and (20) at all gridpoints to machine zero. Therefore, the solid lines of Figs. 5–8 also refer to the present results. More difficult solutions for Re = 1000 and Re = 3200 have also been obtained, using $h = \frac{1}{96}$ and $h = \frac{1}{128}$, respectively, which again coincide with the staggered-grid ones presented in Ref. [7] and are thus omitted for brevity. In all cases the vorticity integral over the entire computational domain was computed and was found to be equal to -1, to machine accuracy.

The Re = 400, $h = \frac{1}{192}$ case has also been used to demonstrate the convergence rate of the method: Figure 9 provides the logarithm of the L_1 norm of the vorticity residual,

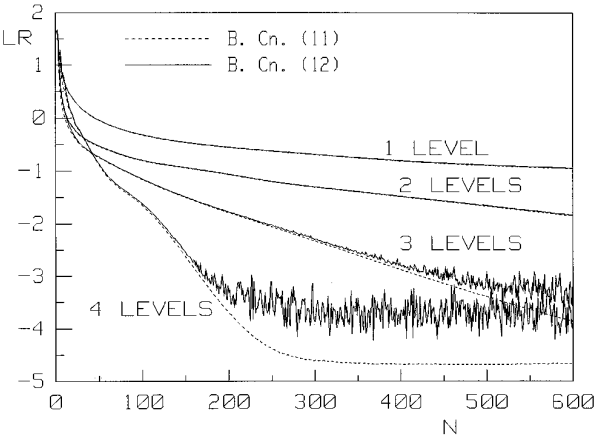

FIG. 9. Convergence histories for Re = 400, $h = \frac{1}{192}$, and different multigrid levels.

LR, versus the number of iterations, N, when using 1, 2, 3, and 4 grid levels, respectively. The broken and solid lines refer to the method of Ref. [6], using Eq. (11), and to the present approach using either procedure for enforcing the new boundary conditions, respectively. It appears that the increased accuracy is obtained without any loss of the convergence rate of the basic relaxation scheme. Only a small increase of the roundoff error (using single precision arithmetic on a HP-APOLLO 735 workstation) is caused by the integral conditioning.

CONCLUSIONS AND FUTURE WORK

For the vorticity–velocity Navier–Stokes equations written as a second-order system on a node-centered uniform Cartesian grid, the proper wall vorticity conditions, capable of providing numerical solutions as accurate as those obtained on a staggered grid, have been found by applying Stokes' theorem to each computational cell adjacent to the boundary. Numerical solutions to the driven cavity flow problem are presented which demonstrate the validity of the proposed approach. Therefore, for the special case considered in this study, the superiority of the staggered-grid discretization for the second-order vorticity–velocity equations has been overcome. The practical usefulness of the proposed conditions requires their extensions to general curvilinear coordinates and three dimensions: both appear to be rather difficult tasks, but are in the authors opinion very worth pursuing.

APPENDIX A

Consider the node-centred second-order-accurate central-difference discretizations of the ω, ψ and ω, u, v equations on a uniform $m \times n$ Cartesian grid. It is proved that, if the numerical solutions to two such sets of equations

provide identical discrete vorticity fields, the discrete solutions for $u_{i,j}$, $v_{i,j}$ are related to the discrete solution for $\psi_{i,j}$ according to Eqs. (17) and (18). In fact, the two discrete vorticity fields being identical, both must satisfy the discrete equations

$$\omega_{i,j} = -\delta^2\psi_{i,j}, \tag{1A}$$

$$\omega_{i,j+1} - \omega_{i,j-1} = -2\Delta y \cdot \delta^2 u_{i,j}, \tag{2A}$$

$$\omega_{i+1,j} - \omega_{i-1,j} = 2\Delta x \cdot \delta^2 v_{i,j}, \tag{3A}$$

$i = 2, ..., m - 1$; $j = 2, ..., n - 1$, where δ^2 indicates the standard five-point Laplacian, namely,

$$\delta^2(\cdot)_{i,j} = \frac{(\cdot)_{i-1,j} - 2(\cdot)_{i,j} + (\cdot)_{i+1,j}}{\Delta x^2} + \frac{(\cdot)_{i,j-1} - 2(\cdot)_{i,j} + (\cdot)_{i,j+1}}{\Delta y^2}.$$

By writing Eq. (1A) at gridpoints (x_i, y_{j+1}) and (x_i, y_{j-1}), subtracting the resulting equations from each other, and eliminating the vorticity terms by means of Eq. (2A), one easily obtains

$$\delta^2\left(u_{i,j} - \frac{\psi_{i,j+1} - \psi_{i,j-1}}{2\Delta y}\right) = \delta^2 f_{i,j} = 0, \tag{4A}$$

where the shorthand notation, $f_{i,j}$, is introduced for convenience. Equation (4A), which is to be satisfied at all interior gridpoints, provides a linear system of $(m - 2) \times (n - 2)$ equations for $m \times n - 4$ unknowns. Furthermore, if all boundaries are no-slip ones, namely lines of constant ψ, and the boundary conditions are imposed according to Eq. (8b), it can be easily seen that system (4A) is made complete by the following homogeneous Dirichlet boundary conditions:

$$f_{1,j} = f_{n,j} = f_{i,1} = f_{i,m} = 0, \quad i = 2, ..., m - 1; j = 2, ..., n - 1. \tag{5A}$$

Such a complete system is well known to possess the unique solution $f_{i,j} = 0$, $i = 2, ..., m - 1$, $j = 2, ..., n - 1$, so that

$$u_{i,j} = \frac{\psi_{i,j+1} - \psi_{i,j-1}}{2\Delta y}, \quad i = 2, ..., m - 1; j = 2, ..., n - 1,$$

which completes the proof sought. Equation (18) is proved in much the same manner, starting from Eq. (3A) instead of Eq. (2A).

APPENDIX B

It is proved that the discrete velocity fields as obtained from the node-centred and staggered-grid second-order-accurate central-difference discretizations of the ω, u, v equations satisfy Eqs. (19) and (20). In fact, with reference to the horizontal velocity components, u, the staggered-grid solutions satisfy the following equations at nodes $(x_i, y_{j+1/2})$ and $(x_i, y_{j-1/2})$, respectively,

$$\frac{\omega_{i,j+1} - \omega_{i,j}}{\Delta y} = -\delta^2 u_{i,j+1/2}, \tag{1B}$$

$$\frac{\omega_{i,j} - \omega_{i,j-1}}{\Delta y} = -\delta^2 u_{i,j-1/2}, \tag{2B}$$

where δ^2 is again the five-point Laplacian. By adding Eqs. (1B) and (2B) one obtains

$$\frac{\omega_{i,j+1} - \omega_{i,j-1}}{\Delta y} = -\delta^2 u_{i,j-1/2} - \delta^2 u_{i,j+1/2} = -\delta^2(u_{i,j-1/2} + u_{i,j+1/2}).$$

Moreover, the node-centred solutions satisfy the discrete form of Eq. (2), namely,

$$\frac{\omega_{i,j+1} - \omega_{i,j-1}}{\Delta y} = -2\delta^2 u_{i,j}.$$

Since the node-centred and staggered-grid solutions to the ω, u, v equations provide identical vorticity fields, one can equate the right-hand sides of the two equations above, which gives

$$\delta^2\left(u_{i,j} - \frac{u_{i,j-1/2} + u_{i,j+1/2}}{2}\right) = \delta^2 f_{i,j} = 0, \quad i = 2, ..., m - 1; j = 2, ..., n - 1. \tag{3B}$$

Moreover, if the no-slip conditions are imposed for the staggered-grid discretization according to Eq. (9a), $f_{i,j} = 0$ at the boundaries. Just like in Appendix A, system (3B), after eliminating the boundary $f_{i,j}$ values, has the unique homogeneous solution, namely,

$$u_{i,j} = \frac{u_{i,j-1/2} + u_{i,j+1/2}}{2}, \quad i = 2, ..., m - 1; j = 2, ..., n - 1.$$

A similar procedure applied to the vertical velocity component, v, allows us to prove Eq. (20).

APPENDIX C

Consider the staggered-grid second-order-accurate central-difference discretizations of the ω, u, v equations. With reference to the grid of Fig. 2, one can write Eq. (21) at nodes (x_i, y_j), (x_{i+1}, y_j), (x_i, y_{j+1}), and (x_{i+1}, y_{j+1}), to obtain

$$\omega_{i,j} = \frac{v_{i+1/2,j} - v_{i-1/2,j}}{\Delta x} - \frac{u_{i,j+1/2} - u_{i,j-1/2}}{\Delta y},$$

$$\omega_{i+1,j} = \frac{v_{i+3/2,j} - v_{i+1/2,j}}{\Delta x} - \frac{u_{i+1,j+1/2} - u_{i+1,j-1/2}}{\Delta y},$$

$$\omega_{i,j+1} = \frac{v_{i+1/2,j+1} - v_{i-1/2,j+1}}{\Delta x} - \frac{u_{i,j+3/2} - u_{i,j+1/2}}{\Delta y},$$

$$\omega_{i+1,j+1} = \frac{v_{i+3/2,j+1} - v_{i+1/2,j+1}}{\Delta x} - \frac{u_{i+1,j+3/2} - u_{i+1,j+1/2}}{\Delta y}.$$

By adding the four equations above one has

$$\begin{aligned}
&\omega_{i,j} + \omega_{i+1,j} + \omega_{i,j+1} + \omega_{i+1,j+1} \\
&\quad = \frac{1}{\Delta x}[(v_{i+1/2,j} + v_{i+3/2,j}) - (v_{i-1/2,j} + v_{i+1/2,j}) \\
&\qquad + (v_{i+1/2,j+1} + v_{i+3/2,j+1}) - (v_{i-1/2,j+1} + v_{i+1/2,j+1})] \\
&\qquad - \frac{1}{\Delta y}[(u_{i,j+1/2} + u_{i,j+3/2}) - (u_{i,j-1/2} + u_{i,j+1/2}) \\
&\qquad + (u_{i+1,j+1/2} + u_{i+1,j+3/2}) - (u_{i+1,j-1/2} + u_{i+1,j+1/2})] \\
&\quad = \frac{2}{\Delta x}(v_{i+1,j} - v_{i,j} + v_{i+1,j+1} - v_{i,j+1}) \\
&\qquad - \frac{2}{\Delta y}(u_{i,j+1} - u_{i,j} + u_{i+1,j+1} - u_{i+1,j}),
\end{aligned}$$

where Eqs. (19) and (20) have been used to introduce the nodal values of the velocity components. A little algebra finally allows us to recover Eq. (22), which is valid for all internal and boundary cells and turns out to be the numerical counterpart of the integral condition (23).

APPENDIX D

Consider the 2D driven cavity flow problem of Fig. 4, the unit square domain being discretized by a uniform $m \times n$ grid, with $\Delta x = 1/(m-1)$ and $\Delta y = 1/(n-1)$. We now prove the validity of one of the four equations (24a)–(24d), namely Eq. (24a). Let us write Eq. (21) at the grid point (2, 2), namely,

$$\omega_{2,2} = \frac{1}{\Delta x}(v_{2+1/2,2} - v_{1+1/2,2}) - \frac{1}{\Delta y}(u_{2,2+1/2} - u_{2,1+1/2}). \tag{1D}$$

Using Eqs. (19) and (20), one easily obtains

$$u_{2,2+1/2} = 2u_{2,2} - u_{2,1+1/2}, \tag{2D}$$

$$v_{2+1/2,2} = 2v_{2,2} - v_{1+1/2,2}. \tag{3D}$$

The continuity equation, written at the corner cell, reads

$$\frac{1}{\Delta x}(u_{2,1+1/2} - u_{1,1+1/2}) + \frac{1}{\Delta y}(v_{1+1/2,2} - v_{1+1/2,1}) = 0. \tag{4D}$$

Since, due to the no-slip boundary condition, $u_{1,1+1/2} = v_{1+1/2,1} = 0$, Eq. (4D) becomes

$$u_{2,1+1/2} = -\frac{\Delta x}{\Delta y} v_{1+1/2,2}. \tag{5D}$$

Consider then Eq. (21) written at node (1, 2):

$$\omega_{1,2} = \frac{1}{\Delta x}(v_{1+1/2,2} - v_{1-1/2,2}) - \frac{1}{\Delta y}(u_{1,2+1/2} - u_{1,1+1/2}). \tag{6D}$$

Since $u_{1,2+1/2} = u_{1,1+1/2} = (v_{1+1/2,2} + v_{1-1/2,2})/2 = v_{1,2} = 0$, due to the no-slip boundary conditions, one easily obtains

$$v_{1+1/2,2} = \frac{\Delta x}{2}\omega_{1,2}. \tag{7D}$$

The staggered-grid velocity components in the right-hand side of Eq. (1D) are finally eliminated by means of Eqs. (2D), (3D), (5D), and (7D), to give

$$\omega_{1,2} = \frac{2(v_{2,2}/\Delta x - u_{2,2}/\Delta y) - \omega_{2,2}}{1 + (\Delta x/\Delta y)^2}. \tag{8D}$$

ACKNOWLEDGMENTS

This research has been supported by M.U.R.S.T. and C.N.R. The authors are grateful to the Associate Editor, J. K. DuKowicz, to the reviewers, and to L. A. Catalano, G. Pascazio, and L. Quartapelle for many interesting criticisms and helpful comments.

REFERENCES

1. H. Fasel, *J. Fluid Mech.* **78,** 355 (1976).
2. S. C. R. Dennis, D. B. Ingham, and R. N. Cook, *J. Comput. Phys.* **33,** 325 (1979).
3. R. K. Agarwal, "A Third-Order-Accurate Upwind Scheme for Navier–Stokes Solutions in Three Dimensions," in *ASME Winter Annual Meeting, 1981* (unpublished).
4. G. Guj and T. Stella, *Int. J. Numer. Methods Fluids* **8,** 405 (1988).
5. P. Giannattasio and M. Napolitano, "Numerical Solutions to the Navier–Stokes Equations in Vorticity–Velocity Form," in *Proceedings, Terzo Convegno Italiano di Meccanica Computazionale, Palermo, Italy, 1988,* (AIMETA, Palermo, Italy, 1988), p. 95.
6. M. Napolitano and L. A. Catalano, *Int. J. Numer. Methods Fluids* **13,** 49 (1991).
7. M. Napolitano and G. Pascazio, *Comput. Fluids* **19,** 489 (1991).

8. G. A. Osswald, K. N. Ghia, and U. Ghia, ''A Direct Algorithm for Solution of Incompressible Three-Dimensional Unsteady Navier–Stokes Equations,'' in *Proceedings, AIAA 8th Computational Fluid Dynamics Conf., Honolulu, HI, 1987* (AIAA, New York, 1987), p. 408.
9. O. Daube, *J. Comput. Phys.* **103,** 402 (1992).
10. P. Giannattasio and M. Napolitano, Internal Report 02/92, Istituto di Fisica Tecnica e di Tecnologie Industriali, University of Udine, Italy, 1992 (unpublished).
11. O. R. Burggraf, *J. Fluid Mech.* **24,** 113 (1966).
12. F. Sotiropoulos and S. Abdallah, *J. Comput. Phys.* **95,** 212 (1991).
13. L. Quartapelle, *Numerical Solution of the Incompressible Navier–Stokes Equations* (Birkhauser Verlag, Basel, 1993), p. 135.